DESIGN AND FABRICATION OF MULTIPURPOSE SMART PHANTOM FOR POSITRON EMISSION TOMOGRAPHY/ COMPUTED TOMOGRAPHY IMAGING

RAFIDAH BINTI ZAINON

UNIVERSITI SAINS MALAYSIA

2008

DESIGN AND FABRICATION OF MULTIPURPOSE SMART PHANTOM FOR POSITRON EMISSION TOMOGRAPHY/COMPUTED TOMOGRAPHY IMAGING

by

RAFIDAH BINTI ZAINON

Thesis submitted in fulfillment of the requirements for the degree of

Master of Science

UNIVERSITI SAINS MALAYSIA

AUGUST 2008

ACKNOWLEDGEMENTS

With the name of Allah, The Most Merciful and The Most Benevolent.

First and foremost my gratitude goes to Allah for giving me an opportunity doing my research study and learns lots of new knowledge. I would like to convey my warmest thanks greeting to my main supervisor, Associate Proffesor Mohamad Suhaimi Jaafar, Professor Ahmad Shukri Mustapa Kamal as my co-supervisor and Dato' Dr Mohamed Ali Kader Shah as my clinical supervisor at Nuclear Medicine Department in Penang GH for giving me much valuable advice and useful guidelines while I'm doing my research study.

Next, I would like to thank the Universiti Sains Malaysia (USM) for support my study in Academic Staff Training Scheme (ASTS). I also wish to thank Advanced Medical and Dental Institute (AMDI), USM for providing me the financial support to fabricate multipurpose smart phantom and practical training at Putrajaya Hospital.

I wish my sincere appreciation to Dr Fadzillah Hamzah, Mr. Mustaffa Hamidon, Mr. Muhd Ludfi Abdul Samat, Ms Noraidawati Embong, Ms Prema Devi a/p Chellayah and the whole staff at Nuclear Medicine Department at Penang GH for their excellence assistance and support during my experiments there.

I would like to convey my thanks to Professor Ahmad Fauzi Mohd Nor, Professor Zainal Arifin Ahmad, Dr Azhar Abu Bakar, Dr Zulkifli Ahmad, Dr Zulkifli Mohamad Ariff at School of Materials & Mineral Resources Engineering, Engineering Campus,

Dr Coswald S. Sipaut @ Mohd Nasri, School of Chemistry, USM, Dr Eid Mahmoud Eid Abdel Munem and Dr Magdy Hussien Mourad Mohamed for their co-operation, encouragement and useful discussion on this research.

Thanks to all technical assistants for their generous help and to all the members of Biophysics and Medical Physics Research Group, School of Physics, thanks for the cooperation and assistance. To my lovely parents, brothers and sisters, thanks so much for their resolute support and encouragement in my life.

CONTENTS

CHAPTER 4: METHODOLOGY OF PREPARATION PHANTOM MATERIALS, DESIGN AND FABRICATION OF NEW PHANTOMS

LIST OF TABLES

LIST OF FIGURES

LIST OF ABBREVIATIONS

Name	Definition
CT	Computed Tomography
MRI	Magnetic Resonance Imaging
2D	Two-dimensional
3D	Three-dimensional
SPECT	Single Positron Emission Tomography
PET	Positron Emission Tomography
PET/CT	Positron Emission Tomography/Computed Tomography
^{18}F-FDG	^{18}F-fluorodeoxyglucose
ROI	Region of Interest
SUV	Standardised Uptake Value
ACR	American College Accreditation
QA	Quality Assurance
QC	Quality Control
FDA	Food and Drug Administration
PMMA	Polymethyl methacrylate
PTFE	Polytetrafluoroethylene
HU	Hounsfield Units
NEMA	National Electrical Manufacturers Association
NIST	National Institute of Standards Technology
LSO	Luthetium-oxyorthosilicate
WB	Whole body
FOV	Field of View

eFOV	Extended Field of View
CTAC	Computed Tomography Attenuation Correction
AC	Attenuation Correction
NIH	National Institutes of Health
ATLAS	Advanced Technology Laboratory Animal Scanner
GE	General Electric
DICOM	Digital Imaging and Communications in Medicine
CPU	Central Processing Unit
SEM	Scanning Electron Microscope
EDX	Energy Dispersive X-ray
H-Vac	High-vacuum
SEI	Secondary-electron Image
WD	Working Distance
BEI	Backscattered-electron Image
L-Vac	Low Vacuum
EOS	Electron Optical System
CL	Condenser Lens
OL	Objective Lens
BMP	Bitmap
TIFF	Tagged Image File Format
JPEG	Joint Photographic Experts Group
CAD	Computer-aided Design
PE	Perkin-Elmer
CHNS	Carbon Hydrogen Nitrogen Sulphur

TCD	Thermal conductivity detector
MCA	Multichannel Analyser
MCB	Multichannel buffer
PC	Personal computer
DC	Direct current
RTD	Rise time discrimination
GUI	Graphical user interface
PP	Polypropylene
MDI	Methylene bisphenyl isocyanate
PE	Polyether
DMCHA	Dimethylcyclohexylamine
PDs	Polydispersity indices
CdTe	Cadmium Tellurium
FWHM	Full Width Half Maximum
CCT	Carbon conductive tabs
ICRU	International Commission on Radiation Units and Measurements

LIST OF SYMBOLS

Name	Definition
Z	Atomic number
σ/ρ	Mass attenuation coefficient of Compton process
E	Energy
τ/ρ	Mass attenuation coefficient of photoelectric process
π/ρ	Mass attenuation coefficient of pair production process
K_e	Kinetic energy of the emitted photoelectron
h	Planck constant
v	Velocity of the electron
E_B	Binding energy of the emitted electron
σ_{ph}	Cross section of photoelectric process
hv	Quantum energy
θ	Electron angle
$2m_0c^2$	The rest mass of the electron-positron pair
E_+	The kinetic energy of positron
E_+	The kinetic energy of electron
E_{nuc}	The kinetic energy of nucleus
ΔI	Transmitted photon beam intensity
I	Incident photon beam intensity
μ_l	Linear attenuation coefficient of the absorber
Δx	The thickness of the absorber
μ_m	Mass attenuation coefficient of the material
μ_l	Linear attenuation coefficient of the material

ρ	Density of the material
μ/ρ	Total mass attenuation coefficient for gamma ray interactions
τ/ρ	Mass attenuation coefficient of photoelectric process
σ/ρ	Mass attenuation coefficient of Compton effect
κ/ρ	Mass attenuation coefficient of pair production
ΔN	Numbers of atoms of the nuclide in the sample present at a time, t
Δt	Time
λ	Decay constant
A	Activity of the nuclide (disintegrations/second)
λ	Decay constant (s^{-1})
$N(t)$	Number of atoms at a time, t
N_0	Number of atoms initially present
λ	Decay constant
t	Time
$t_{1/2}$	Half-life
μ_T	Linear attenuation coefficient of tissue
μ_{water}	Linear attenuation coefficient of water
g	Gram
Bq	Becquerel
MBq	Mega Becquerel
GBq	Giga Becquerel
ml	Millilitre
kg	kilogram
Ge	Germanium

Ci	Curie
mCi	Milicurie
γ	Gamma
Gy	Gray
V	Volt
keV	Kiloelectron Volt
MeV	Megaelectron Volt
dps	Decays per second
dpm	Decays per minute
s	Second
nm	Nanometre
mW	Miliwatt
µm	Micrometre
mm	Milimetre
mA	Miliampere
kVp	Peak kilovoltage
K	Kelvin
pA	Picoampere
µA	Microampere
Pa	Pascal
Hz	Hertz
kVA	Kilovolt ampere
CO_2	Carbon dioxide
H_2O	Water

N_2	Nitrogen
SO_2	Sulphur dioxide
μg	Micro gram
$CaCO_3$	Calcium Carbonate
ºC	Degree Celsius
ºF	Degree Fahrenheit
w%	Weight percentage
^{241}Am	Americium-241
X	Magnification
psi	Pound per square inch
F-18	Flourine-18
I_o	Flux of incident photons
I_{trans}	Flux of transmitted photons through a thickness

LIST OF APPENDICES

DESIGN AND FABRICATION OF MULTIPURPOSE SMART PHANTOM FOR POSITRON EMISSION TOMOGRAPHY/COMPUTED TOMOGRAPHY IMAGING

ABSTRACT

Phantom studies are an important part in medical imaging as it can evaluate the performance and quality assurance (QA) test of dual-modality PET/CT. The purpose of this study is to design, fabricate and develop a multipurpose smart phantom which includes the internal structures, water, human tissue equivalent materials and radioactive source for dual-modality Positron Emission Tomography/Computed Tomography (PET/CT) imaging. In this study, experimental determination of Hounsfield units (HU), mass attenuation coefficient, elemental composition analysis and structure analysis were performed on phantom materials using PET/CT scanner, Multichannel Analyser (MCA), CHNS analyser and Scanning Electron Microscope/Energy Dispersive X-Ray (SEM/EDX) respectively. From these analyses, the fabricated inserts of epoxy, polyurethane and paraffin wax were found to be equivalent to human spongy bone, lung and soft tissue respectively. The CT numbers of these inserts were +220.094 HU, -949.725 HU and -115.499 HU respectively. Besides, other properties of these phantom materials had been identified and were compared with human tissues. These fabricated inserts together with PMMA and PTFE were then selected for the designed and fabrication of a multipurpose smart phantom. PET/CT performance tests carried out on the phantom demonstrated that the fabricated phantom can be utilised as a phantom for PET/CT imaging for various types of human tissues.

REKABENTUK DAN FABRIKASI FANTOM PINTAR PELBAGAI TUJUAN UNTUK PENGIMEJAN TOMOGRAFI PANCARAN POSITRON/ TOMOGRAFI BERKOMPUTER

ABSTRAK

Kajian fantom adalah bahagian yang penting dalam pengimejan perubatan kerana ia dapat menilai perlaksanaan dan ujian jaminan kualiti (QA) dwi-modaliti Tomografi Pancaran Positron/Tomografi Berkomputer (PET/CT). Tujuan kajian ini adalah untuk merekabentuk, memfabrikasi dan membangunkan fantom pintar pelbagai tujuan yang termasuk struktur dalaman, air, bahan-bahan setara dengan tisu manusia dan sumber radioaktif untuk pengimejan dwi-modaliti PET/CT. Dalam kajian ini, penentuan secara eksperimen Unit Hounsfield (HU), pekali atenuasi jisim, analisis komposisi elemen dan analisis struktur telah dilakukan terhadap bahan-bahan fantom menggunakan PET/CT skan, Penganalisis Berbilang Saluran (MCA), Penganalis CHNS dan Pengimbas Mikroskop Elektron/Keselerakan Tenaga X-ray (SEM/EDX) masing-masing. Daripada analisis ini, fabrikasi epoksi, poliuretin dan lilin paraffin didapati masing-masing setara dengan tulang lembut manusia, paru-paru dan tisu lembut. Nombor-nombor CT bahan-bahan ini adalah +220.094 HU, -949.725 HU dan -115.499 HU masing-masing. Selain itu, ciri-ciri lain bahan-bahan ini juga dikenalpasti dan dibandingkan dengan tisu manusia. Bahan-bahan yang difabrikasi ini bersama dengan PMMA dan PTFE kemudian telah dipilih untuk rekabentuk dan fabrikasi fantom pintar pelbagai tujuan. Ujian perlaksanaan PET/CT yang dijalankan ke atas fantom menunjukkan bahawa fantom yang difabrikasi boleh dimanfaatkan sebagai fantom untuk pengimejan PET/CT bagi pelbagai jenis tisu manusia.

CHAPTER 1: INTRODUCTION

1.1 BACKGROUND

Medical imaging of the human body requires some form of energy. In the medical imaging techniques used in radiology, the energy used to produce the image must be capable of penetrating tissues. The electromagnetic spectrum outside the visible light region is used for X-ray imaging, including mammography, Computed Tomography (CT), magnetic resonance imaging (MRI) and in nuclear medicine. Mechanical energy in the form of high-frequency sound waves is used in ultrasound imaging. The advances in medical imaging and computerised medical image processing have led to new two-dimensional (2D) and three-dimensional (3D) imaging modalities that have become important clinical tools in diagnostic radiology. The clinical significance of radiological imaging modalities in diagnosis and treatment of diseases is overwhelming.

Several modern imaging modalities are in practice today to acquire anatomical, physiological, metabolic and functional information from the human body. The commonly used medical imaging modalities capable of producing multidimensional images from radiological diagnostic applications are: X-ray CT, Single Positron Emission Tomography (SPECT), Positron Emission Tomography (PET) and ultrasound. These modern imaging methods involved sophisticated instrumentations and equipments using high-speed electronics and computers for data collection, image reconstruction and display. The recent complex medical imaging modalities depend heavily on computer technology for creation and display of digital images.

Using computers, multidimensional digital images of physiological structures can be processed and manipulated to visualise hidden characteristic diagnostic features that are difficult or impossible to see with planar imaging methods. Furthermore, these features of interest can be quantified and analysed using sophisticated computer programs and models to understand their behavior to help with a diagnosis or to evaluate treatment protocols. Imaging methods available today for radiological applications may use external, internal or a combination of energy sources. In most commonly used imaging methods, ionised radiation imaging such as X-rays are used as an external energy source primarily for anatomical imaging. Such anatomical imaging modalities are based on attenuation coefficient of radiation passing through the body.

For example, X-ray radiographs and CT imaging modalities measure attenuation coefficients of X-ray that are based on density of the tissue or part of the body being imaged. Another example of external energy source based imaging is ultrasound or acoustic imaging. With the exception of nuclear medicine, all medical imaging requires that the energy used to penetrate the human body's tissue also interact with those tissues. If energy were to pass through the body and some type of interaction such as absorption, attenuation and scattering occurs, then the detected energy would contain useful information regarding the internal anatomy and thus it would be possible to construct an image of the anatomy using that information. In nuclear medicine imaging, radioactive agent is injected or ingested and it is metabolic or physiologic information of the agent that gives rise to the information in the images.

This imaging modalities use an internal energy source through an emission process to image the human body. For emission imaging, the injected radioactive pharmaceuticals are interacting with selected body matter or tissue to form an internal source of radioactive energy that is used for imaging. The emission process and energy range of γ-rays cause limitations on the resolution and data acquisition time for imaging. This emission imaging principle is applied in PET and SPECT. Such types of nuclear medicine modalities provide useful metabolic information about the physiological functions of the organ. Further, a good combination of external stimulation on internal energy sources can be used in medical imaging to acquire more accurate information about the tissue material and physiological responses and functions.

In recent years, technological advances enabled the development of a new scanner that combines PET and CT into one machine. The result is an entirely new picture in the science of diagnostic imaging providing a far more complete picture of a patient's overall health. Positron Emission Tomography/Computed Tomography (PET/CT) is unique imaging technologies that visualise abnormalities within the body. Each yields very different information and the two modalities have been used in conjunction in the diagnosis, treatment and follow-up of cancer. Unlike conventional imaging procedures that measure the structure of an abnormality, PET measures the metabolic changes that occur in cells when disease is present. The atoms, molecules and cells of our body have particular behaviors and chemical processes. At the onset of disease, these behaviors change, often before a detectable physical difference like a tumor occurs. This is because cancer cells behave differently than normal cells. PET technology can detect these subtle changes and identify cancer at its most basic cellular level.

On the other hand, PET is limited in that it does not give the size or shape of the abnormality. Thus, CT scan procedures will perform this task. It combines X-ray technology with advanced computer acquisition to uncover the precise form and location of an abnormality. CT is one of the primary tools of measurement in oncology evaluation. It is extremely fast and yields minutely thin slices, cross-sectional views of the body. The new PET/CT scanner acquires both pictures during the same exam. Sophisticated software then fuses the images. The result is a full body view showing the presence or absence of disease, how active it is, whether or not it is spread and precisely where and how large an abnormality is. In addition to diagnosis and staging, the PET/CT scan is essential in re-staging or detecting remaining cancer cells after the patients had undergone treatment. Besides, the PET/CT imaging also performs one image which shows all the organ systems and it can shows how the body respond to treatment.

A safe, short-lived radiopharmaceutical, known as ^{18}F-fluorodeoxyglucose (^{18}F-FDG) is used in PET/CT scan studies. This is related to the high standardisation and relative ease of synthesis of this tracer, to the relatively long half-life of ^{18}F which allows distribution of FDG in human body and to its well known biological behaviour. ^{18}F-FDG is tagged to a glucose molecule because cancer cells are highly metabolic and use more glucose than normal cells, hence the increased glucose activity is measured. Mostly, ^{18}F-FDG is supplied in isotonic saline as a sterile, non-pyrogenic, clear, colourless solution and it is used for diagnostic radiopharmaceutical for PET. The calculated activity is related to Standardised Uptake Value (SUV) and is reported as an absolute number.

It is now considered the most accurate clinical staging study for non-small-cell lung cancer and is also important in the staging of other multiple malignancies (Black, Quinten C. *et al.,* 2004). ^{18}F-FDG decays by positron emission and has a half life of 110 minutes. The principal photons useful for diagnostic imaging are the 511 keV gamma photons, resulting from the interaction of the emitted positron with an electron. This radiopharmaceutical had been injected into the phantom to evaluate PET image quality which includes ROI analysis, SUV analysis and so on. American College Accreditation (ACR) had provided an instruction for PET phantom for routine evaluation of PET/CT systems.

Phantom is a tissue substitute of any material that simulates a body of tissue in its interaction with ionising or non-ionising radiation. It can be any structure that contains one or more tissue substitutes and in the case of radiographic phantom, it is used to simulate radiation interactions in the human body. A phantom allows the effects of an imaging system on receptor quantification to be investigated under conditions very similar to those in a patient. It can be used to optimise the imaging system for patient imaging and to examine information about the procedure such as estimated dosage given. Phantom studies are used to perform numerous tasks and an important part in diagnostic imaging quality as it can evaluates the performance and quality assurance (QA) test of imaging modalities. Besides, phantoms are often used to demonstrate the relationship between objects scanned and their final images.

Water tanks were often used for X-ray experiments and till now these materials are still in use in certain applications. Currently, the use of tissue equivalent materials has

increased over the years. There are a number of material substitutes which is equivalent to tissues of human organs or body parts such as polyester (Brain W. *et al.,* 2006), polystyrene (Joel Y. C. Cheung *et al.,* 2002), polyethylene (Jessi Clements *et al.,* 2002), epoxy resin (Jessi Clements *et al.,* 2002; Brain W. *et al.,* 2006) and polymethyl methacrylate (PMMA) (Joel Y. C. Cheung *et al.,* 2002; Parodia K *et al.,* 2007). Much research has been carried out to find the most suitable tissue equivalent material in diagnostic radiology (Christopher J. Bachler *et al.,* 2006), radiotherapy (Lavely *et al.,* 2004) and radiation protection (G. Dietze*,* 2000; J. I. Kim *et al.,* 2006).

Since phantoms are designed to mimic tissue, they are typically composed of materials that act like tissue. Ideally, the phantom material substitutes must have the same density and the same mass attenuation coefficient properties with those of human tissues being simulated. The mass attenuation coefficient is a measure that describes how much radiation will attenuate in a material and it is dependent on the density of the absorbing material. In PET/CT imaging, phantom study plays an essential part in medical imaging as this dual purpose imaging device can shows the metabolic or chemical activity in the body and the anatomical structures of human body. The individual scans, which are taken virtually consecutively, can be presented separately or as a single, overlapping or fused image.

Quality control (QC) of CT consists of imaging a phantom and checking for CT number. This QC need to make sure that the CT numbers are accurately calibrated. The energy calibration on the CT scanner at 120 kVp, 100 kVp, or 140 kVp will generate the attenuation maps that are used for PET purposes. Besides, for PET side the QC of it is

performed, the activity injected, time and issues such as that are need to be considered in order to improve diagnostic accuracy in common cancers. The ability to do PET imaging allows us to identify cancer cells, if they are present, more accurately over the traditional methods such as CT which are dependent on imaging the anatomy. So PET essentially visualise metabolism and function. Consequently, this study can be done on phantom which will overcome some of the problems encountered in QC tests and it gives more information about the result acquired from the medical imaging modalities.

1.2 RESEARCH PROBLEM

At present, there are a number of commercially available PET/CT test phantoms for measuring daily QC tests and periodic, comprehensive QC testing to meet the requirements of the Food and Drug Administration (FDA), United States. In any case, test phantoms are often considered difficult, tedious or requiring special software, in addition to cost-effectiveness problems. Previously, the available existing phantom is simplistic with only few tissue equivalent materials, usually made of polytetrafluoroethylene (PTFE), air, water and it is limited to certain tissues equivalent only.

Although PET/CT imaging offers many advantages, this dual-modality imaging also possesses some challenges. The interpretation of PET/CT images is very important to make use of the available data, and at very least, provide an interpretation of the precise location and anatomical relationships of ^{18}F-FDG abnormalities (Wechalekar K. *et al.*, 2005). These reasons have been the force behind the efforts to develop a practical, handy and cheap phantom.

On the same note, there is an urgent need to study phantoms to evaluate the image quality in whole-body PET/CT imaging. Consequently, to design a new test phantom that would combine simplicity with quality to facilitate the evaluation of PET/CT systems.

1.3 OBJECTIVES OF RESEARCH

The main objectives of this research can be summarised as follows:

1. To design, fabricate and develop a multipurpose smart phantom which includes the internal structures, water, human tissue equivalent materials and radioactive source for PET/CT imaging.
2. To analyse the properties of manufactured and fabricated phantoms materials and comparison with human tissues.
3. To study the PET/CT performance tests using fabricated multipurpose smart phantom.

1.4 SCOPE OF RESEARCH

In this study, suitable existing and new fabricated materials will be identified to test for suitability as tissue equivalent materials for PET/CT imaging. The phantom will be designed and fabricated using the identified materials which are equivalent to human tissues with appropriate CT numbers. Furthermore, a radioactive source will be inserted in this phantom to evaluate the PET/CT performance test on the multipurpose smart phantom.

1.5 THESIS ORGANISATION

In this section, the contents of the successive chapters will be described. In Chapter 2, the discussion will focus on fundamentals of interaction of radiation with matters. Besides, it also reviews the current research relevant to this study. In Chapter 3, a description of equipments that have been used in this research will be presented.

Next, the methodology of this study will be discussed in Chapter 4. In this chapter, the discussion will focus on preparation of phantom materials, tests for manufactured and fabricated phantom materials, fabrication of new phantoms and PET/CT performance tests. Besides, in Chapter 5 the discussion will focus on results and discussions which include the results obtained from phantom materials tests, analysis of selected phantom materials and results of PET/CT performance test.

Last but not least, the conclusion and further work will be summarised in Chapter 6. Finally, it will be followed by references, appendices and list of publications.

CHAPTER 2: THEORY AND LITERATURE REVIEW

2.1 FUNDAMENTALS OF INTERACTION OF RADIATION WITH MATTER

High-energy photons (gamma rays, X-rays, annihilation radiation and *Bremsstrahlung*) transfer their energy to matter in complex interactions with atoms, nuclei and electrons. However, these interactions can be viewed as a simple collision between a photon and a target atom, nucleus or electron. These interactions do not cause ionisation directly, as do the charged particle interactions. Some of the photons interactions result in the injection of orbital electrons from atoms or in the creation of positive-negative electron pairs. These electrons in turn cause ionisation effects, which are the basis for mechanisms by which high-energy photons are detected and by which they cause radiobiologic effects. For these reasons, high-energy photons are classified as secondary ionising radiation. The selective interactions of X-ray photons with the structure of the human body produces the image; the interaction of photons with the receptor converts an X-rays or gamma rays image into one that can be viewed or recorded.

There are five types of interactions with matter by X-ray and gamma ray photons; Compton effect, photoelectric effect, pair production, Rayleigh (coherent) scattering and photonuclear interactions. The first three of these are the most important, as they result in the transfer of energy to electrons, which then impart that energy to matter in many (usually small) Coulomb-force interactions along their tracks. The relative importance of Compton effect, photoelectric effect and pair production depends on both the photon

quantum energy and the atomic number, Z of the absorbing medium as shown in Eq. 2.1, 2.2 and 2.3.

$$\frac{\sigma}{\rho} \propto \frac{\text{electron density}}{E} \qquad 2.1$$

Where: σ/ρ = Mass attenuation coefficient of Compton process
E = Energy

$$\frac{\tau}{\rho} \propto \frac{Z^3}{E^3} \qquad 2.2$$

Where: τ/ρ = Mass attenuation coefficient of photoelectric process
Z = Atomic number
E = Energy

$$\frac{\pi}{\rho} \propto (E - 1.02)\, Z \qquad 2.3$$

Where: π/ρ = Mass attenuation coefficient of pair production process
E = Energy
Z = Atomic number

2.1.1 PHOTOELECTRIC PROCESS

In this process, an incident photon striking an atom ejects one of the orbital electrons of the atom (Figure 2.1). During this absorption the gamma ray disappears, its entire energy being given up.

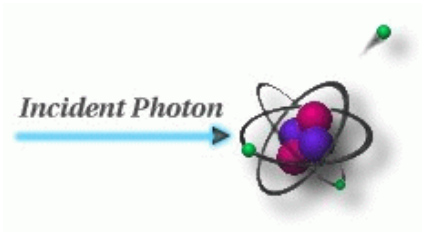

Figure 2.1 Schematic representation of the photoelectric effect.
(Taken from Sprawls Educational Foundation)

The kinetic energy, K_e of the emitted photoelectron is shown in Eq. 2.4. The photoelectron could be emitted from the K-shell, L-shell, etc., of the atom. The photoelectric process will take place only if $h\nu > E_B$.

$$K_e = h\nu - E_B \qquad 2.4$$

Where: K_e = Kinetic energy of the emitted photoelectron
h = Planck constant
v = Velocity of the electron
E_B = Binding energy of the emitted electron

After the atomic electron is ejected by a photoelectric effect, the vacancy in that shell is filled up by another electron from the outer shell. This is followed by emission of X-rays or Auger electrons consuming the binding energy E_B. The configuration of the atomic shell recovers within a very short time after the photoelectric emission. The atomic X-rays absorbed by the matter surrounding the point of emission, giving rise to further electrons. Thus the total energy of the incident gamma ray is completely converted into the kinetic energy of the electrons. The cross section for photoelectric effect has been calculated and it depends on $h\nu$ and Z according to Eq. 2.5.

$$\sigma_{ph} \propto \frac{Z^5}{(h\nu)^{7/2}} \qquad 2.5$$

Where: σ_{ph} = Cross section of photoelectric process
Z = Atomic number
$h\nu$ = Quantum energy

2.1.2 COMPTON SCATTERING

Compton scattering occurs when the incident X-ray photon interacts with a free electron and is scattered with a loss of energy. Compton scattering also includes scattering of photons by electrons bound to an atom because in comparison to the energy of the photon, the electron binding energy is quite small (Figure 2.2).

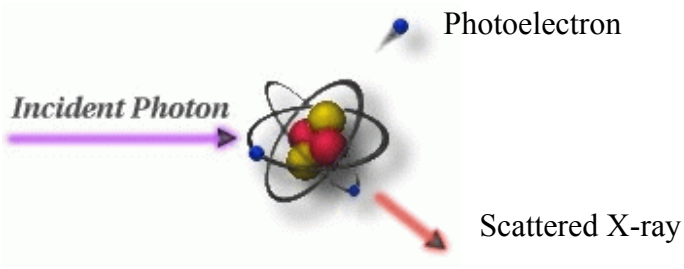

Figure 2.2 Schematic representation of Compton scattering.
(Taken from Sprawls Educational Foundation)

Thus, an incident photon of energy $h\nu$ can be considered to collide with a free electron of rest mass m_0. The photon is scattered through an angle θ with an energy $h\nu'$ ($< h\nu$) while the electron recoils with a kinetic energy K_e at an angle ϕ. Application of laws of conservation of linear momentum and energy with relativistic expressions gives the expressions as shown in Eq. 2.6.

$$h\nu' = \frac{h\nu}{1 + \alpha\,(1 - \cos\theta)} \qquad 2.6$$

Where: $h\nu$ = Photon energy
θ = Electron angle

2.1.3 PAIR PRODUCTION

Pair production is a direct conversion of radiant energy to matter. For pair production to occur, the electromagnetic energy, in a discrete quantity called a photon, must have energy greater than 1.02 MeV strikes a material of high *Z*, it is found that the photon is completely absorbed and a pair of electron and positron is produced (Figure 2.3).

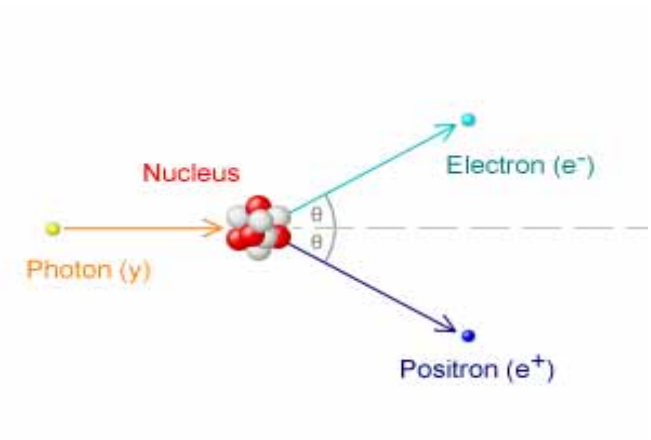

Figure 2.3 Kinematics of pair production process.
(Taken from Sprawls Educational Foundation)

The threshold energy of the photon is 1.02 MeV. The conversion of energy yields as shown in Eq. 2.7. The presence of the nucleus is essential for the conversion of linear momentum.

$$h\nu = 2m_0c^2 + E_+ + E_- + E_{nuc} \qquad 2.7$$

where
$h\nu$ = The incident photon energy
$2m_0c^2$ = The rest mass of the electron-positron pair
E_+ = The kinetic energy of positron
E_+ = The kinetic energy of electron
E_{nuc} = The kinetic energy of nucleus

2.1.4 RAYLEIGH (COHERENT) SCATTERING

Rayleigh scattering is called coherent because the photon is scattered by the combined action of the whole atom. The event is elastic in the sense that the photon loses essentially none of its energy; the atom moves just enough to conserve momentum. The photon is usually redirected through only a small angle.

Therefore the effect on a photon beam can only be detected in narrow-beam geometry. Rayleigh scattering has more practical importance at low energies, partly because the scattering angle is greater. The relative importance of this process is seen to be fairly small, as it contributes only a few percent or less of the narrow-beam attenuation coefficient.

2.1.5 PHOTONUCLEAR INTERACTIONS

Photonuclear reactions are one of the methods for generating radionuclide. These reactions require minimum photon energy of about 2 MeV and they are not significant in most elements until photon energies exceed about 10 MeV. Also, even at these energies, the probability of photonuclear reactions is much smaller than that of Compton scattering or pair production. Furthermore, the effective total sum of attenuation coefficients is the total sum of attenuation coefficient of photoelectric absorption and Compton scattering. Therefore, photonuclear reactions are of no practical importance in terms of photon beam attenuation or the transfer of photon energy to matter.

2.2 ATTENUATION OF PHOTON BEAM

When a photon passes through a thickness of absorber material, the probability that it will experience an interaction depends on its energy and on the composition and thickness of the absorber (Figure 2.4).

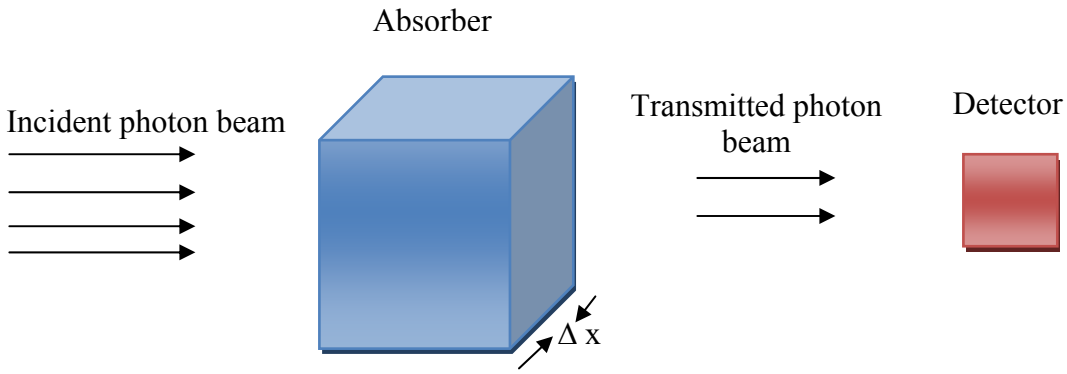

Figure 2.4 Photon beam transmission.
(Taken from Sprawls Educational Foundation)

Consider a beam of photons of intensity I (photons/cm^2.sec) directed onto an absorber of thickness Δx. Due to composition and photon energy effects, it will be assumed for the moment that the absorber is comprised of a single element of atomic number, Z and that the beam is monoenergetic with energy E. A photon detector records transmitted beam intensity. The fractional decrease in beam intensity $\Delta I/I$ is related to absorber thickness Δx as shown in Eq. 2.8. The minus sign indicates beam intensity decreases with increasing absorber thickness.

$$(\Delta I/I) = -\mu_l \Delta x \qquad 2.8$$

Where: ΔI = Transmitted photon beam intensity
I = Incident photon beam intensity
μ_l = Linear attenuation coefficient of the absorber
Δx = The thickness of the absorber

The quantity of μ_l is found to increase linearly with absorber density ρ. Density effects are factored out by dividing μ_l by density ρ as shown in 2.9. The mass attenuation coefficient of the material has dimensions cm^2/g. It depends on the Z of the absorber and photon energy E. The total mass attenuation coefficient for gamma ray interactions, neglecting photonuclear interactions can be written in units of $cm^2.g^{-1}$ as shown in Eq. 2.10.

$$\mu_m = \mu_l / \rho \qquad 2.9$$

Where: μ_m = Mass attenuation coefficient of the material
μ_l = Linear attenuation coefficient of the material
ρ = Density of the material

$$\frac{\mu}{\rho} = \frac{\tau}{\rho} + \frac{\sigma}{\rho} + \frac{\kappa}{\rho} \qquad 2.10$$

Where: μ/ρ = Total mass attenuation coefficient for gamma ray interactions
τ/ρ = Mass attenuation coefficient of photoelectric process
σ/ρ = Mass attenuation coefficient of Compton effect
κ/ρ = Mass attenuation coefficient of pair production

2.3 DECAY OF RADIOACTIVITY

Radioactivity decay is a spontaneous process; there is no way to predict uncertainty the exact moment at which an unstable nucleus will undergo its radioactive transformation into another, more stable nucleus. Radioactive decay is described in terms of probabilities and average decay rates.

2.3.1 DECAY CONSTANT

The average decay rate of a sample containing N radioactive atoms of a certain radionuclide is as shown in Eq. 2.11. The decay constant has a characteristic value for each radionuclide. It is the fraction of the atoms in a sample of that radionuclide undergoing radioactive decay per unit of time during a time period that is so short that only a small fraction decay during that interval. The unit of λ is s^{-1}.

$$\Delta N / \Delta t = - \lambda N \qquad 2.11$$

Where: ΔN = Numbers of atoms of the nuclide in the sample present at a time, t
Δt = Time
λ = Decay constant
N = Number of atoms of the nuclide in the sample initially present

2.3.2 DEFINITIONS AND UNITS OF ACTIVITY

The quantity $\Delta N/\Delta t$, the average decay rate is the activity A of the sample. It has dimensions decays per second (dps) or decays per minute (dpm) and is essentially a measure of how radioactive the sample is. The S.I unit of activity is Becquerel (Bq). The equation of activity for a sample is as shown in Eq. 2.12.

$$A \text{ (Bq)} = \lambda N \qquad 2.12$$

Where: A = Activity of the nuclide (disintegrations/second)
λ = Decay constant (s^{-1})
N = Number of atoms of the nuclide in the sample

2.3.3 EXPONENTIAL DECAY

With the passage of time, the number N of radioactive atoms in a sample decreases. Therefore, A of the sample also decreases. Figure 2.5 illustrates the radioactive decay with the passage of time.

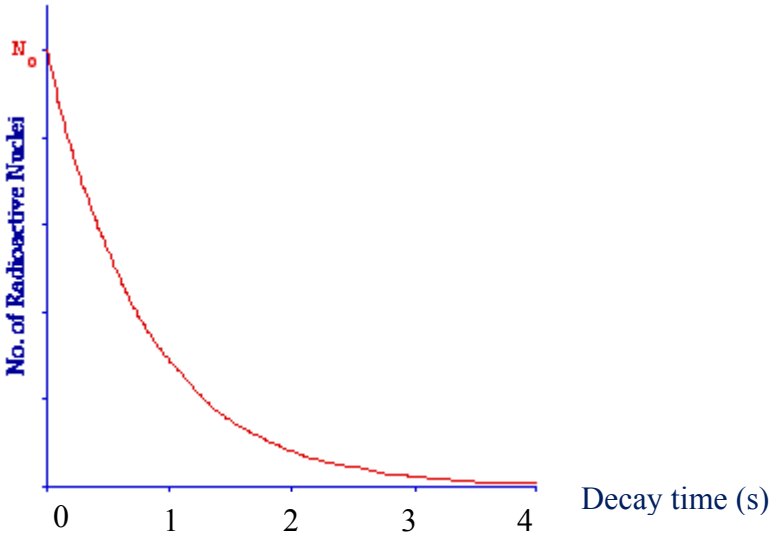

Figure 2.5 Decay of radioactive sample during successive 1 s increment of time. (Taken from Integrated Publishing's Archive Service, 2007)

The number of atoms remaining after a time, t is as shown in Eq. 2.13. Since A is proportional to N, the decay factor also supplies to activity versus time as shown in Eq. 2.14.

$$N(t) = N_0 e^{-\lambda t} \qquad 2.13$$

Where: $N(t)$ = Number of atoms at a time, t
N_0 = Number of atoms initially present
λ = Decay constant
t = Time

$$A(t) = A_0 e^{-\lambda t} \qquad 2.14$$

Where : $A(t)$ = Activity present at time, t
A_0 = Activity initially present
λ = Decay constant
t = Time

2.3.4 RADIOACTIVITY HALF-LIFE

One of the most useful terms for estimating how quickly a nuclide will decay is the radioactive half-life. The radioactive half-life is defined as the amount of time required for the activity to decrease to 50% of its initial activity level. A relationship between the half-life and decay constant can be developed from Eq. 2.15.

$$A(t) = A_0 e^{-\lambda t} \qquad 2.15$$

$$ln\left(\frac{A}{A_0}\right) = -\lambda t$$

$$t = \frac{ln\left(\frac{A}{A_0}\right)}{\lambda}$$

The half-life can be calculated by solving Eq. 2.14 for the time, t, when the current activity, A, equals one-half the initial activity A_0. Substituting this in the Eq. 2.15 above yields an expression for $t_{1/2}$ as shown in Eq. 2.16.

$$t_{1/2} = -\frac{\ln\left(\frac{1}{2}\right)}{\lambda} \qquad 2.16$$

$$t_{1/2} = \frac{\ln 2}{\lambda} = \frac{0.693}{\lambda}$$

Figure 2.6 shows radioactive decay as a function of time in units of half-life. An initial number of atoms N_0, the population, and consequently, the activity may be noted to decrease by one-half of this value in a time of $t_{1/2}$. Additional decreases occur so that whenever $t_{1/2}$ elapses; the number of atoms drops to one-half of what its value was at the

beginning of that time interval. After five half-lives have elapsed, only 1/32, or 3.1%, of the original number of atoms remains. After seven half-lives, only 1/128, or 0.78%, of the atoms remains. The number of atoms existing after 5 to 7 half-lives can usually be assumed to be negligible.

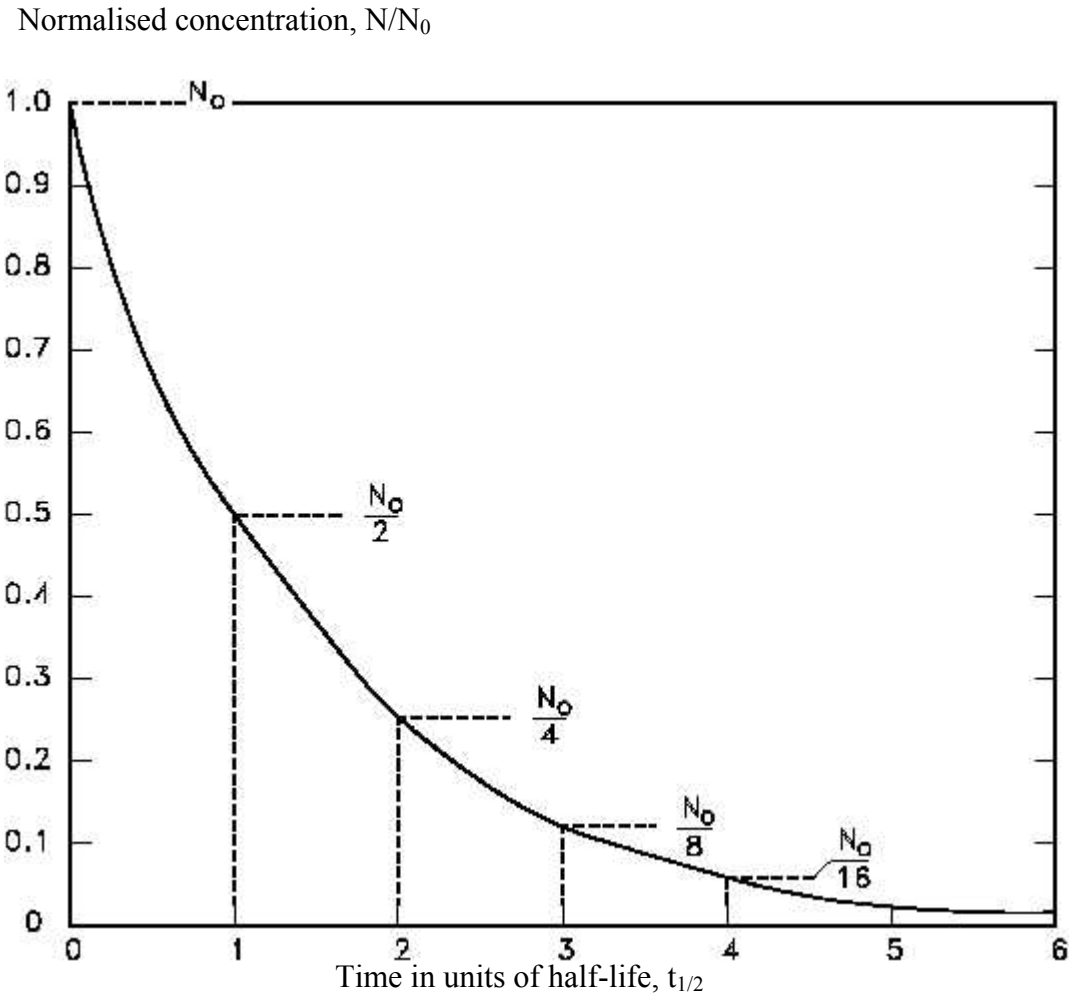

Figure 2.6 Radioactive decay as a function of time in units of half-life.
(Taken from Integrated Publishing's Archive Service, 2007)

The lifetimes of individual radioactive atoms in a sample range anywhere from very short to very long. Some atoms decay almost immediately, whereas a few do not decay

for relatively long time. The average lifetime τ of the atoms in a sample has a value that is characteristic of the nuclide and is related to the decay constant λ as shown in Eq. 2.17.

$$\tau = 1/\lambda \qquad 2.17$$

Where: τ = Average lifetime
λ = Decay constant

2.4 CT NUMBERS

CT numbers is also known as Hounsfield units (HU). The reconstruction of algorithm generates CT numbers which are related to attenuation coefficients. The CT numbers range from -1000 HU for air to +1000 HU for bone, water and consequently each water-equivalent tissue with $\mu_T = \mu_{water}$ has the value 0 HU. For an arbitrary tissue T with attenuation coefficient μ_T the CT values is defined as in Eq. 2.18

$$H = (\mu_T - \mu_{water}) / \mu_{water} \text{ x } 1000 \text{ HU} \qquad 2.18$$

Where: H = Hounsfield unit or CT number
μ_T = Linear attenuation coefficient of tissue
μ_{water} = Linear attenuation coefficient of water

An increase in CT values can be assigned to increased density or an increase in effective atomic number. This corresponds to the physical definition of the linear attenuation coefficient as shown in Eq. 2.19.

$$\mu = (\mu / \rho)\ (E, Z).\ \rho \qquad 2.19$$

Where: μ = Linear attenuation coefficient
ρ = Density
E = Energy
Z = Atomic number

2.5 SUV OF ^{18}F-FDG

The most widely used semiquantitative index in PET studies is the SUV which represents an index for FDG accumulation in tissue. This can be calculated as the ratio between the FDG uptake (MBq/ml) in a small ROI (placed over the tumour in an attenuation-corrected image) and the administered activity to the weight (kg) or body surface (m^2) of the patient. The equation of SUV is as shown in Eq. 2.20.

$$SUV = \frac{\text{Tissue concentration (MBq/g)}}{\text{Injected dose (MBq) / body weight (g)}} \qquad 2.20$$

A calibration factor is required to convert the value measured from the image into MBq/ml. SUVs should be calculated in the hottest part of the lesion because cancer tissues have a very heterogeneous distribution of FDG uptake. Calculation of the SUV requires all available data on patient characteristics (weight, height, blood glucose levels) and injected radiopharmaceutical (injected activity of FDG, preparation time and administration time).

2.6 LITERATURE REVIEW

2.6.1 Phantom

Paul E. Kinahan *et al.* (2007) studied on a calibration phantom for multi-centre and longitudinal PET/CT studies of assessing response to therapy. The phantom is based on the National Electrical Manufacturers Association (NEMA) NU-2 IQ phantom, with six hot spheres (internal diameters of 10 mm, 13 mm, 17 mm, 22 mm, 28 mm, and 37 mm) as target lesions. The phantom uses Ge-68 to remove filling variability and allow for estimating standard errors and reproducibility. Absolute quantitation is obtained by

using a National Institute of Standards Technology (NIST) traceable source for the Ge-68 calibration phantom. The effect of lesion size is measured by the six spheres. The overall activity level is based on a 10-15 mCi injection in a 70 kg patient, with sphere:background ratio set to 4:1. The resulting images analysed in terms of mean and max absolute activity and SUV vary with sphere diameter.

Ruiz-Trejo *et al.* (2005) concentrated on a study of design and construction of CT phantom. A phantom for performance evaluation and quality assurance of CT scanners was designed and built in agreement with quality control requirements established by the Mexican Regulations. Phantom materials were chosen after experimental determination of their Hounsfield units. The phantom allows performing the following tests: calibration, constancy and uniformity of the CT number. CT number dependence on the reconstruction algorithm, high and low contrast resolution, slice thickness and coincidence of the slice with the light system for patient alignment. Image quality assessment for CT exams was performed using a commercially two different CT scanners.

C. B. Chiarot *et al.* (2005) studied on development, characterisation, and QA of advanced X-ray imaging technologies which require phantoms that are quantitative and well suited to such modalities. This note reports on the design, construction, and use of an innovative phantom developed for advanced imaging technologies (e.g. multi-detector CT and the numerous applications of flat-panel detectors in dual-energy imaging, tomosynthesis, and cone-beam CT) in diagnostic and image guided procedures. The design addresses shortcomings of existing phantoms